

CONCEPTUAL DESIGNS FOR IR OPTICS AT C0

**JOHN A. JOHNSTONE
FERMILAB**

JUNE 15th, 2000

CONTENTS

1. General Considerations.....	1
2. An IR with High-Field Dipoles.....	1
2.1. Physical Design.....	1
2.1.1. Quadrupoles	1
2.1.2. Dipoles & Separators	3
2.2. Optics	3
2.2.1. B0, C0, & D0 Low- β^* Squeezes	4
2.2.1.1. $\beta^* = 4.00$ @ C0 - (β_x^* , β_y^*) = (1.61, 1.74) @ B0 & D0.....	5
2.2.1.2. $\beta^* = 4.00$ @ C0 - $\beta^* = 0.35$ @ B0 & D0.....	6
2.2.1.3. $\beta^* = 0.50$ @ C0 - (β_x^* , β_y^*) = (1.61, 1.74) @ B0 & D0	7
2.2.1.4. $\beta^* = 0.50$ @ C0 - $\beta^* = 0.35$ @ B0 & D0.....	8
2.3. Beam Separation.....	10
3. An IR with Standard Tevatron Dipoles.....	13
3.1. Physical Design.....	13
3.1.1. Quadrupoles	13
3.1.2. Dipoles & Separators	13
3.2. Optics	14
3.3. Beam Separation.....	15
3.3.1. C0 Without Collisions.....	16
3.3.2. C0 With Collisions.....	16
3.4. Collisions at B0, C0, & D0	17
4. Summary & Observations.....	19

1. GENERAL CONSIDERATIONS

Given the advanced state of operational plans for Run IIb (132 nsec bunch spacing) a new C0 Interaction Region (IR) insertion should be capable of operating in a manner that does not impact nominal Run IIb Tevatron parameters. This implies creating an entirely localized insertion – one which is completely transparent to the rest of the machine. This constraint has several important design implications, some of which are pointed out below.

- An IR design similar to that employed at CDF & D0 is unacceptable as a C0 candidate. The addition of such a (single) low- β region to the machine raises the tune by a half-integer in each plane, moving them far from the standard operating point and smack onto the 21.0 integer resonance. The nominal (fractional) tunes are most elegantly maintained by adding 2 low- β 's locally in each plane, thereby boosting the machine tunes by a full integer.
- The B0 & D0 IR's are not optically-isolated entities. Progression through the low- β squeeze involves adjusting, not only the main IR quadrupoles, but also the tune quad strings distributed around the ring. The result is that the lattice functions at any point in the ring, and the phase advances across any section of the ring, are not fixed quantities, but vary through the squeeze sequence. The C0 IR optics must be sufficiently flexible to track these elusive matching conditions.
- With collisions only at B0 & D0 the unit transfer matrix added by the C0 insert ensures that the incoming & outgoing helices are automatically matched into the established Run IIb values. To maintain this match with collisions at all 3 IP's, however, requires that additional separators be added in the arcs. Space for these separators can only be generated by replacing standard Tevatron arc dipoles with new magnets having enhanced field strengths.

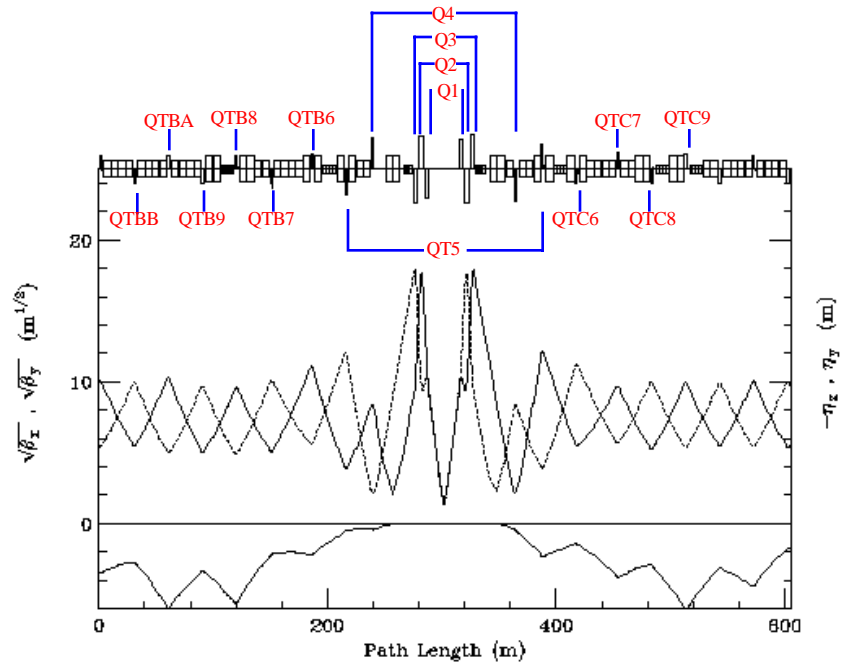
In subsequent sections two variations of an interaction region design are presented. The first of these, which incorporates stronger dipoles, fulfills all the ideal design criteria outlined above. The result is a truly independent 3rd Tevatron IR capable of supporting simultaneous collisions at all 3 IP's. The second, stripped-down, version includes neither stronger dipoles nor new arc separators. While this insert is also optically transparent to the machine, useful collisions can only occur at B0 & D0, or just C0, but not all three. The restriction to standard-strength dipoles also results in a significant reduction of the space available for a detector.

2. AN IR WITH HIGH-FIELD DIPOLES

2.1. Physical Design

2.1.1. Quadrupoles

Both the series & independent IR quad circuits are illustrated below. The new magnets required fall into 3 gradient ranges. There are LHC-like magnets operating in the vicinity of 180 T/m. This is substantially less than the >220 T/m LHC design, but the gradients are limited in this application by the Tevatron 4.2K cryogenics. High-field 140 T/m quadrupoles, modeled like existing magnets installed at the other 2 IR's, are also used. And there are high gradient (≥ 60 T/m) correction spools which, again, are comparable to those at CDF & D0.



Composition of the quadrupole circuits is described below, with the indicated lengths being magnetic lengths:

Q1	:	93"	LHC
Q2	:	160"	LHC
Q3	:	93"	LHC

Unlike the triplets at B0 & D0, the inner & outer quadrupole circuits (Q1 & Q3) of the final focus in this model are powered separately.

Q4	[B48 / C12]	:	66"	LHC
----	---------------	---	-----	-----

The Q4 quads are accompanied by short (56") spoils containing just dipole correctors & BPM's in both planes.

Q5 & Q5T	[B47 / C13]	:	55.19"	140 T/m
		:	25"	60 T/m

The regular 66" arc quads plus their spoils at B47 & C13 are replaced by high field 55" magnets, operating at a constant 136 T/m, plus a series connection of tunable strong correctors for focusing adjustments.

QTB6 & QTC6		:	25"	60 T/m
QTB7 & QTC7	[B45 / C15]	:	23.875"	140 T/m

At B45 & C15 the Tevatron 66" arc quads and their short spoils are replaced by (existing) 32" magnets powered on the main buss plus very strong, independently-powered correctors like those currently installed at the A47, B13, C47, & D13 locations ¹.

¹ This configuration actually increases (by 5") the space available for power feeds.

All the remaining trim quad spools – QTBB8 → QTBB, and QTC8 & QTC9 – are of the 25", strong, 60 T/m variety.

Non-standard separations appear between some of the insertion's inner arc quadrupoles. Between the B48 & B47 [C12 & C13] quadrupoles space is reduced from 4 to 3 dipoles, whereas between B46 & B45 [C14 & C15] separation increases by 1 dipole slot length. Extensive simulations have shown this configuration contributes markedly to the robustness of the IR's optical versatility.

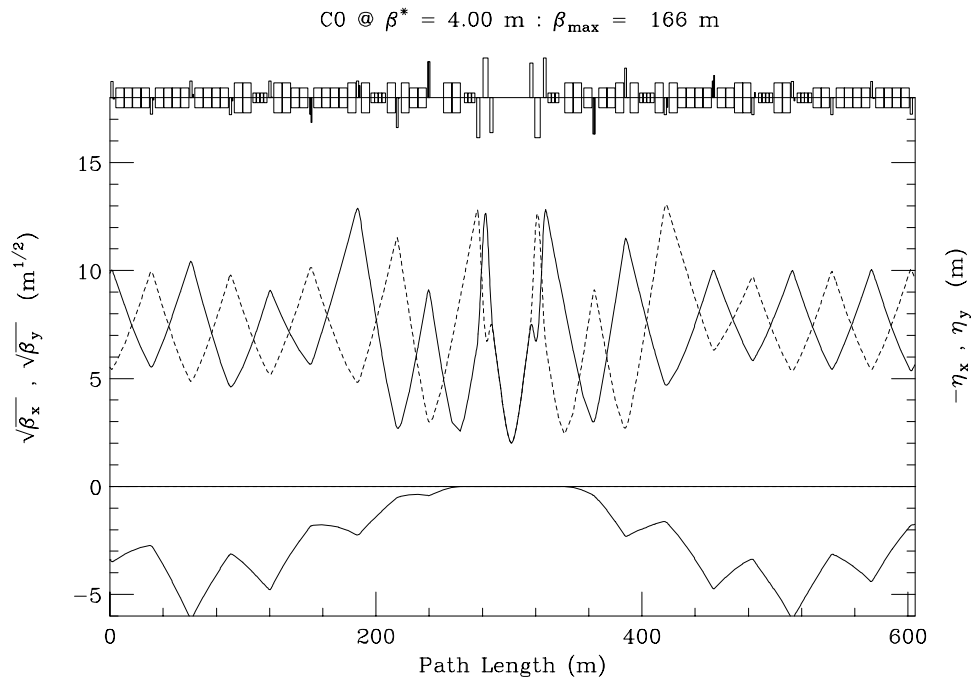
Trim quads are allocated in a lop-sided configuration, with 2 more installed in the upstream end of the insert. In B-sector it is possible to extend insert elements a good distance back into the arc before interfering with Run IIb operations. Not so in C-sector. The 4 vertical separators at C17 are integral components of Run IIb controls and, therefore, define the downstream insert boundary.

2.1.2. Dipoles & Separators

A total of 30 standard Tevatron dipoles are replaced by 20 high-field dipoles. This has two substantial benefits ². First, additional longitudinal space for the detector is generated by installing extra strength bends in the vicinity of the IP. In the current design there is >13 m of free space each side of the IP. Second, by replacing 12 standard dipoles with 8 stronger ones in the B- & C-sector arcs, sufficient space is created between B43 & B44 [C16 & C17] to install 4 separators, and another 4 between B46 & B47 [C13 & C14].

There are 3 separators each side of the IP, immediately outboard of the triplets, for controlling beam position at the IP. New arc separators are necessary both for angle control at the IP and for matching the incoming to outgoing helix. Without these the 3 IR's can not operate independently.

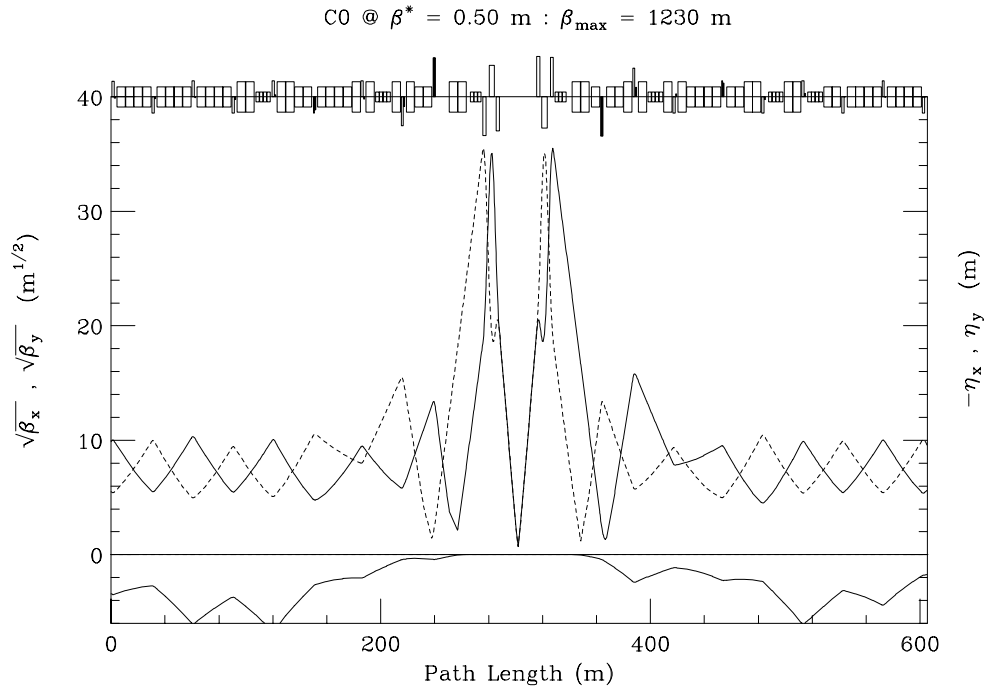
2.2. Optics



² A 3rd, lesser, bonus is that the Tevatron orbit shrinks by about 11 mm – helping somewhat to alleviate the infamous 4 cm circumference mismatch between the Main Injector & Tevatron.

In the injection lattice, shown above, $\beta^* = 4.00$ m results in a β_{\max} of only 166 m in the triplets. This is considerably less than the >240 m of the B0 & D0 injection lattices, and not too much larger than the 120 m of a standard Collins insert.

Tevatron Collider experience suggests that the smallest realistic β^* attainable is limited by the good-field aperture and, therefore, β_{\max} in the low- β triplets, rather than by any gradient limitations of the IR quads. In the current model the Q1 magnets at C0 are roughly 20' farther from the IP than the corresponding ones at B0 & D0. As a result, β_{\max} is considerably larger at C0 for any given value of β^* . With $\beta^* = 50$ cm, β_{\max} has already grown to 1230 m. This is somewhat larger ($\sim 12\%$) than the β_{\max} for $\beta^* = 35$ cm at the other IP's, but is probably still acceptable.



2.2.1. B0, C0, & D0 Low- β^* Squeezes

There are 16 optical constraints the insertion must satisfy. The 6 incoming Twiss parameters are matched at the IP to $\beta_x^* = \beta_y^* \equiv \beta^*$, $\alpha_x^* = \alpha_y^* \equiv 0$, $\eta^* \equiv 0$, $\eta'^* \equiv 0$, and then matched back into the nominal arc values at the downstream end of the insert (at C17). The fractional Run IIb phase shifts, $\Delta\mu_x$ and $\Delta\mu_y$, are preserved across the insert. The final constraint imposed is the insistence that $\beta_{\max}(x) = \beta_{\max}(y)$ in the triplets on each side of the IP. While this last restriction isn't really crucial, it is the best choice, minimizing the consumption of aperture in the low- β quads.

In the design discussed here, every stage of the squeeze from $\beta^* = 4.00 \rightarrow 0.50$ m at C0 can match exactly to any step in the Injection $\rightarrow \beta^* = 0.35$ m squeeze at B0 & D0. The following pages illustrate the lattice functions & tabulate the C0 quadrupole gradients corresponding to the extremes of this operational matrix:

- (1) $\beta^* = 4.00$ @ C0 - $(\beta_x^*, \beta_y^*) = (1.61, 1.74)$ @ B0 & D0
- (2) $\beta^* = 4.00$ @ C0 - $\beta^* = 0.35$ @ B0 & D0

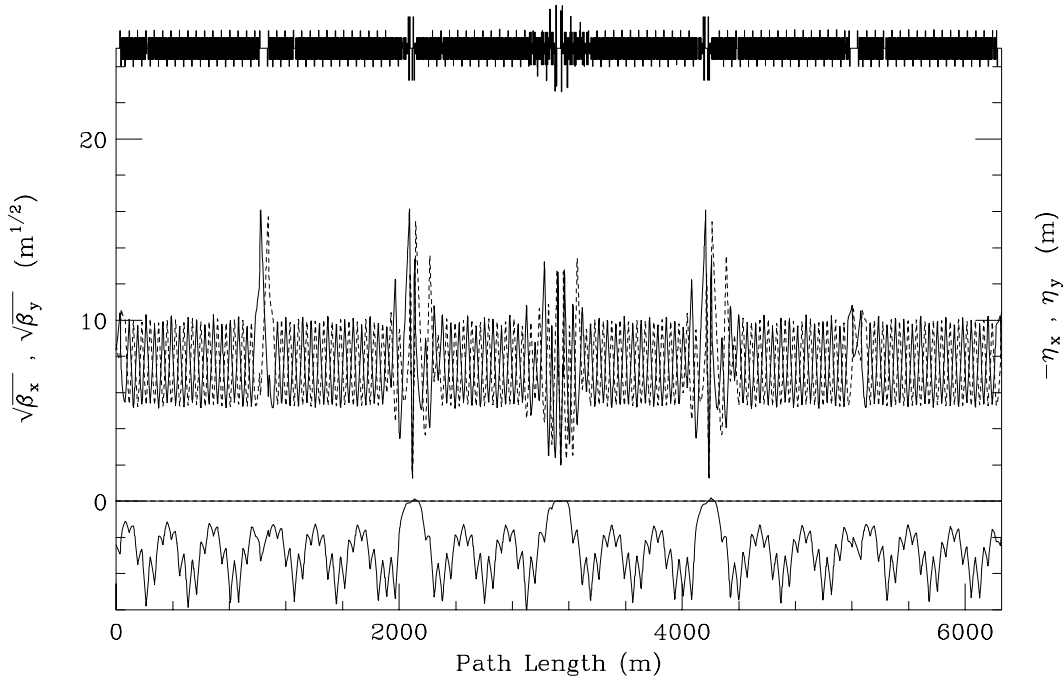
(3) $\beta^* = 0.50 @ C0 - (\beta_x^*, \beta_y^*) = (1.61, 1.74) @ B0 \& D0$

(4) $\beta^* = 0.50 @ C0 - \beta^* = 0.35 @ B0 \& D0$

All gradients in the following tables reflect 1 TeV/c operations. Highlighted entries indicate magnets that change polarity at some point during the squeezes.

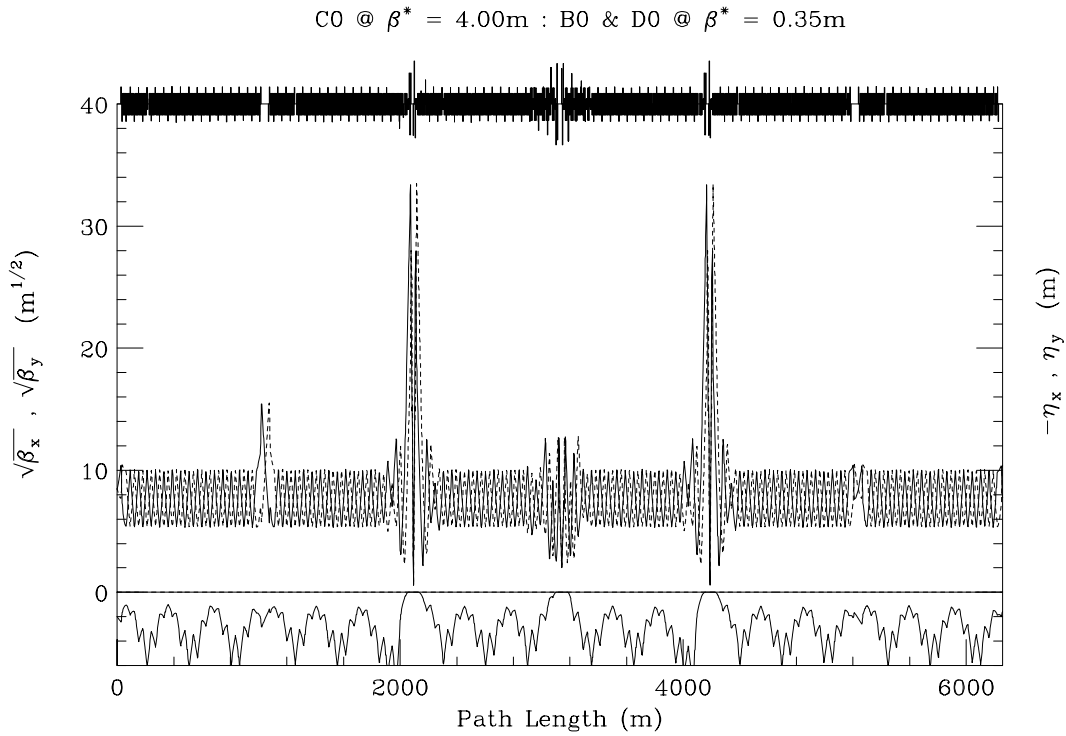
2.2.1.1. $\beta^* = 4.00 @ C0 - (\beta_x^*, \beta_y) = (1.61, 1.74) @ B0 \& D0$

C0 @ $\beta^* = 4.00m : B0 \& D0 @ INJECTION$



Quad #	C0 @ $\beta^* = 4.00 m$ B0 & D0 @ $(\beta_x^*, \beta_y^*) = (1.61, 1.74)$	
	up	down
Q1	-159.197	159.197
Q2	182.773	-182.773
Q3	-180.026	180.026
Q4	165.415	-165.415
QT5	-5.380	5.380
QT6	61.267	-50.421
QT7	-116.421	110.525
QT8	0.192	22.098
QT9	-12.545	-16.572
QTA	16.989	
QTB	-18.316	

2.2.1.2. $\beta^* = 4.00$ @ C0 – $\beta^* = 0.35$ @ B0 & D0



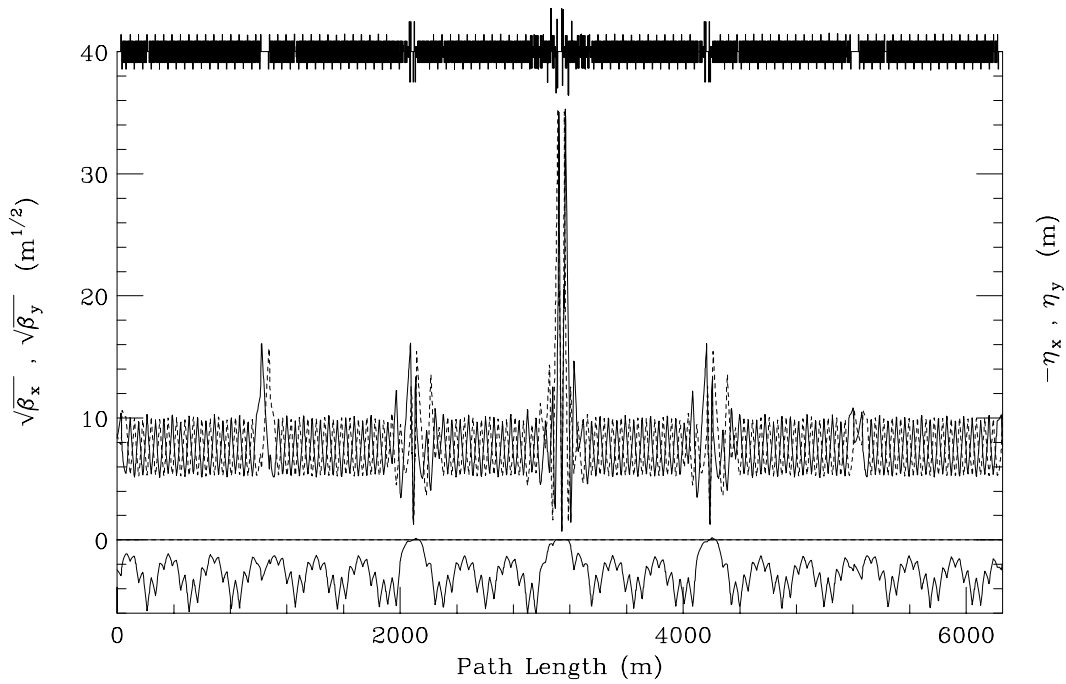
Quad #	C0 @ $\beta^* = 4.00$ m B0 & D0 @ $\beta^* = 0.35$ m	
	up	down
Q1	-158.808	158.808
Q2	182.161	-182.161
Q3	-181.170	181.170
Q4	165.529	-165.529
QT5	-1.755	1.755
QT6	54.929	-43.812
QT7	-113.596	101.506
QT8	3.083	23.788
QT9	-14.645	-13.484
QTA	15.655	
QTB	-9.758	

The 2 preceding tables listed C0 IR gradients corresponding, for example, to the endpoints of an operating scenario in which β^* at C0 is fixed at 4.00 m while β^* at B0 & D0 is squeezed from the Injection values $\rightarrow \beta^* = 0.35$ m for collisions. At each step of this low- β squeeze the C0 magnets are adjusted to maintain the optical match to the 'appropriate', ever-changing lattice functions & phase advances across the insert. The following table indicates the extent to which these gradients vary during the B0 & D0 squeeze.

	B' [max] T/m	B' [min] T/m	$\Delta \int B' \bullet ds$ T-m/m
Q1	159.505	158.893	1.44
Q2	183.764	182.767	3.97
Q3	180.667	179.156	3.57
Q4	159.547	158.745	1.35
QT5	1.381	0.347	0.66
QTB6	63.996	58.866	3.26
QTB7	117.517	115.112	1.46
QTB8	7.761	5.048	1.72
QTB9	13.138	7.625	3.50
QTBA	15.779	13.099	1.70
QTBB	17.448	10.205	4.60
QTC6	60.315	51.426	5.64
QTC7	114.890	106.930	4.83
QTC8	9.449	8.265	0.75
QTC9	17.613	13.113	2.86

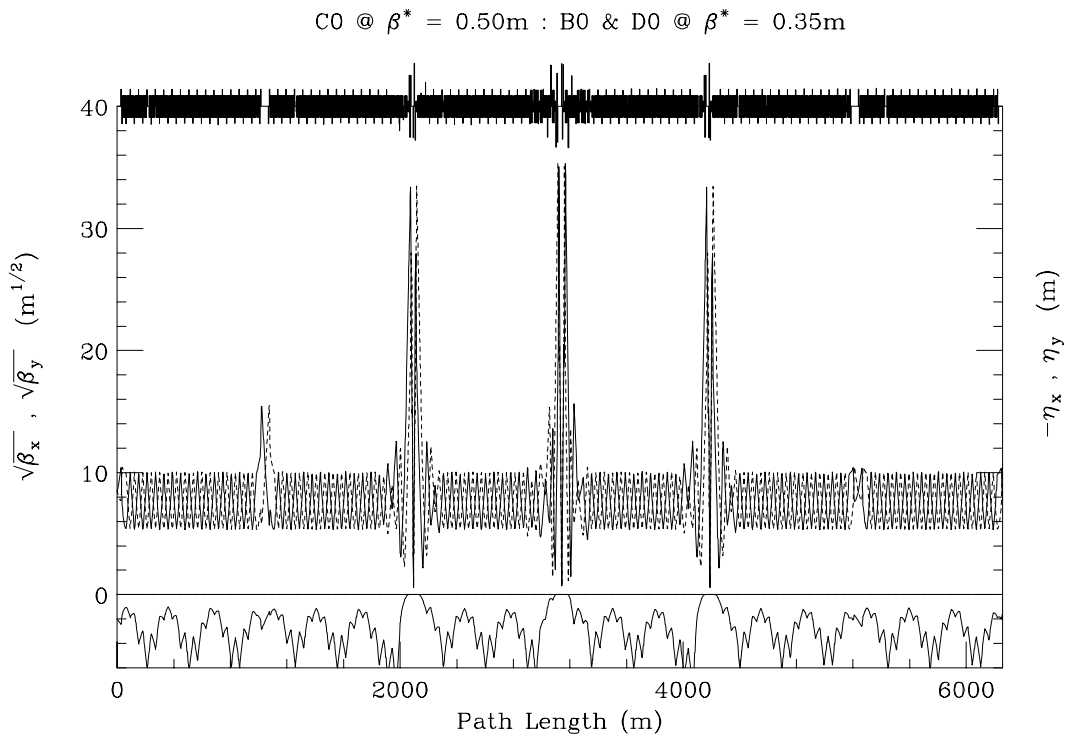
2.2.1.3. $\beta^* = 0.50$ @ C0 - $(\beta_x^*, \beta_y^*) = (1.61, 1.74)$ @ B0 & D0

C0 @ $\beta^* = 0.50m$: B0 & D0 @ INJECTION



Quad #	C0 @ $\beta^* = 0.50$ m	
	B0 & D0 @ (β^*_x, β^*_y) = (1.61, 1.74) up	down
Q1	-159.787	159.787
Q2	179.807	-179.807
Q3	-180.416	180.416
Q4	191.400	-191.400
QT5	-52.248	52.248
QT6	2.849	-6.700
QT7	-67.307	80.573
QT8	8.930	-20.630
QT9	-9.832	19.694
QTA	-1.100	
QTB	-12.828	

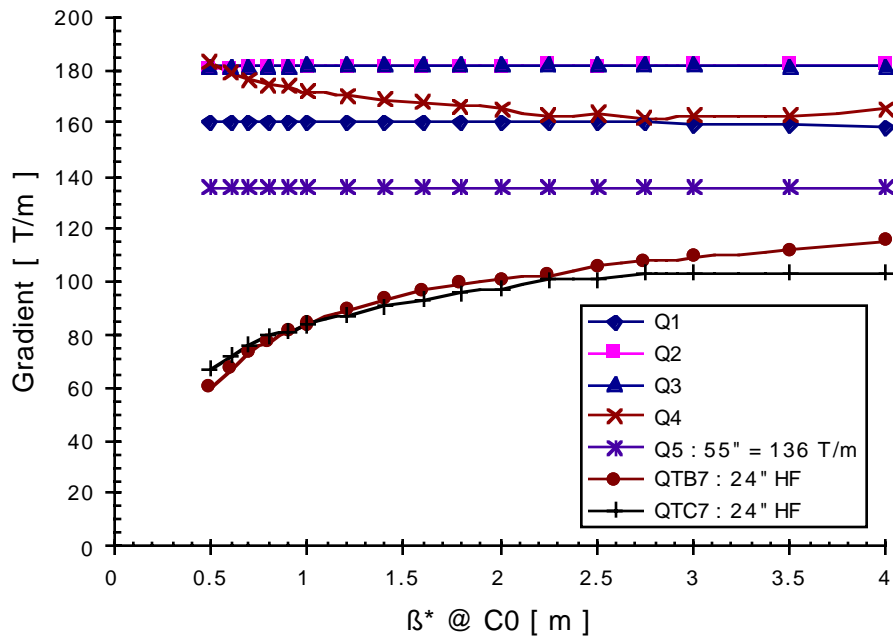
2.2.1.4. $\beta^* = 0.50$ @ C0 – $\beta^* = 0.35$ @ B0 & D0



Quad #	C0 @ $\beta^* = 0.50$ m	
	up	down
Q1	-160.126	160.126
Q2	180.398	-180.398
Q3	-180.909	180.909
Q4	184.500	-184.500
QT5	-45.193	45.193
QT6	-9.753	14.561
QT7	-62.911	65.942
QT8	9.292	-9.253
QT9	-16.317	17.486
QTA	-2.099	
QTB	-11.577	

With β^* at B0 & D0 fixed at 0.35 m, the following graph shows the variation of the high-field quad gradients through a C0 squeeze from $\beta^* = 4.00$ m \rightarrow $\beta^* = 0.50$ m.

High-Field Quad Gradient Variations with β^*
 [B0 & D0 @ $\beta^* = 0.35$ m]



It is important that the new insertion has the optical versatility to match between all the conceivable combinations of β^* at the 3 IR's. While it is imagined that all 3 IR's will operate at low- β simultaneously, it is unlikely that they will be squeezed in tandem. It is well known that between each step of the B0 & D0 low- β squeeze a quadratic tune shift appears. By the sequential squeezing of B0 & D0, followed by C0 (or vice versa), this problem isn't compounded unnecessarily.

2.3. Beam Separation

To reduce the number of interactions per crossing at the IP's, it is planned in Run IIb to reduce bunch spacing in the Tevatron from 396 \rightarrow 132 nsec. With the first parasitic crossings then occurring just 19.86 m from the IP's, though, it is realized that crossing angles must be introduced to obtain separated beams at these points³.

Collider operation with crossing angles has at least 2 major consequences. First, luminosity is reduced due to the decreased overlap of the beams at the IP. A compromise must therefore be reached between minimizing the beam-beam tune shift from the first parasitic crossings (large $\theta_{1/2}$) & minimizing the luminosity reduction (small $\theta_{1/2}$). The second impact of crossing angles is to produce separated beams in the low- β final-focus quadrupoles – precisely where β already reaches its ring-wide maximum. With head-on collisions the Collider currently operates with $\beta^* = 35$ cm, and β_{\max} in the triplets is then ~ 1100 m. It is generally suspected (though not verified) that the minimum β^* attainable is limited by the adverse impact on the beam by high-order multipoles in the low- β quadrupoles. The consequences of sending beams off-axis through the magnets as well is not well understood – the Tevatron has never been operated before with crossing angles.

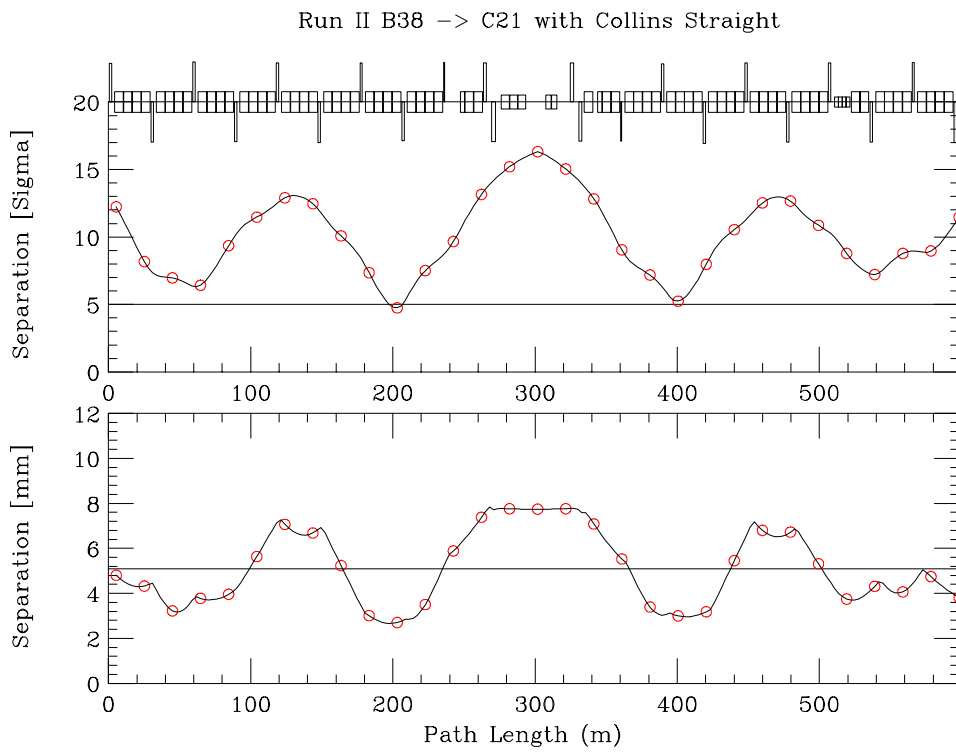
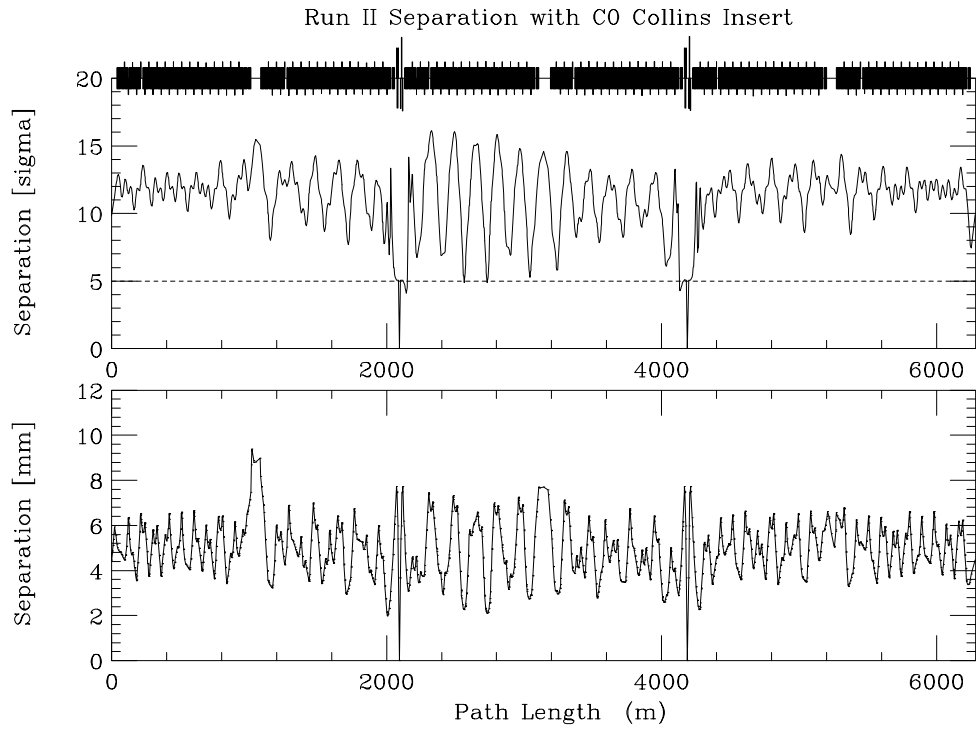
Beyond the decisions to implement shorter bunch spacing & crossing angles in Run IIb, many details of collision scenarios have not been finalized. Significantly, for instance, there is no 'official' helix to describe Collider operations in this era – several promising candidates exist – and the final locations of separators have not yet been established. The collision helix assumed for the purposes of the current study should be viewed, therefore, as only the latest *helix du jour*, and might be quite different in detail from the eventual configuration. In this version⁴ the half-crossing angles at B0 & D0 are $(x^*, y^*) = (+170, -170)$ μrad , giving 5σ of separation at the 1st crossing for $\beta^* = 35$ cm, and 20π emittance (95%, normalized) beams.

This particular incarnation of the Run IIb helix, unfortunately, is not well-suited for also supporting collisions at C0. Beam separation, with the standard Collins insert at C0 still installed, is shown in the following figures. Separation is clearly poorest in the short B0 \rightarrow C0 \rightarrow D0 arc, dipping near to 5σ in several locations. Furthermore, the illustration of just the B38 \rightarrow C21 section suggests it will be difficult for a new IR insertion to create comfortable beam separation in the vicinities of the minima at B47 & C13, while maintaining the requisite match to the nominal helix.

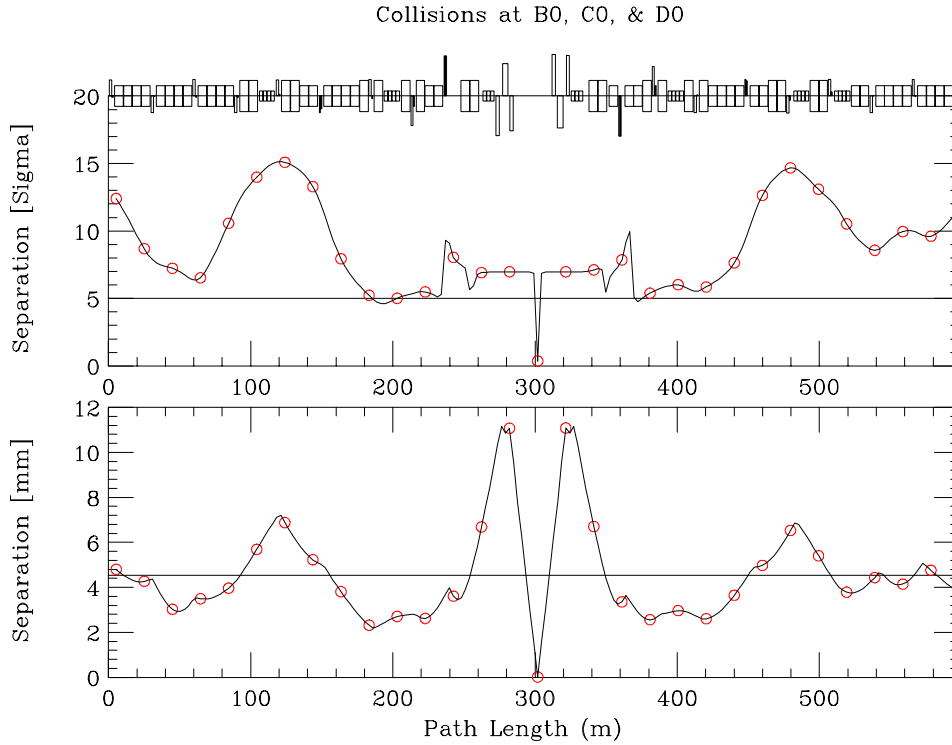
New arc separators in this model have been situated to optimize beam separation, consistent with this one, specific, Run IIb helix solution. With separators at B43, B46, C13, and C16, collisions can be created at all 3 IP's while matching to the nominal incoming & outgoing helices across the C0 insert. (It is also possible to have collisions at just B0 & D0, or just C0, of course. Discussion of these less interesting operational modes is postponed, however, until the next section where, in the 2nd IR version, these become the only operational choices).

³ 132 nsec Bunch Spacing in the Tevatron Proton-Antiproton Collider, S.D. Holmes, *et al.*, TM-1920.

⁴ "v3h15acsb4.nppn.170pnpn", Peter Bagley, private communication.



Shown below is the beam separation from B38 → C21. At the IP, $\beta^* = 0.50$ m and there are half-crossing angles of $(x'^*, y'^*) = (-195, +195)$ μrad , giving 7σ separation at the first parasitic crossings. Other potential collision points are indicated, spaced at 7 half-bucket intervals. The separation is generally acceptable but, as anticipated, is poorest each side of the IP – hovering near 5σ until outboard of the 6th secondary crossing points around B46 & C14.



The large crossing angles ($275 \mu\text{rad}$ total half-angle) are necessary to keep the beams adequately separated through the natural minima of the Run IIb helix. However, the impact on luminosity is at least no worse here than the crossing angle effect at B0 & D0. A crossing angle reduces the luminosity relative to that of head-on collisions, L_0 , by the factor:

$$L_\theta = \left[1 + \left(\theta_{1/2} \cdot \frac{\sigma_{\parallel}}{\sigma_{\perp}} \right)^2 \right]^{-1/2} \cdot L_0$$

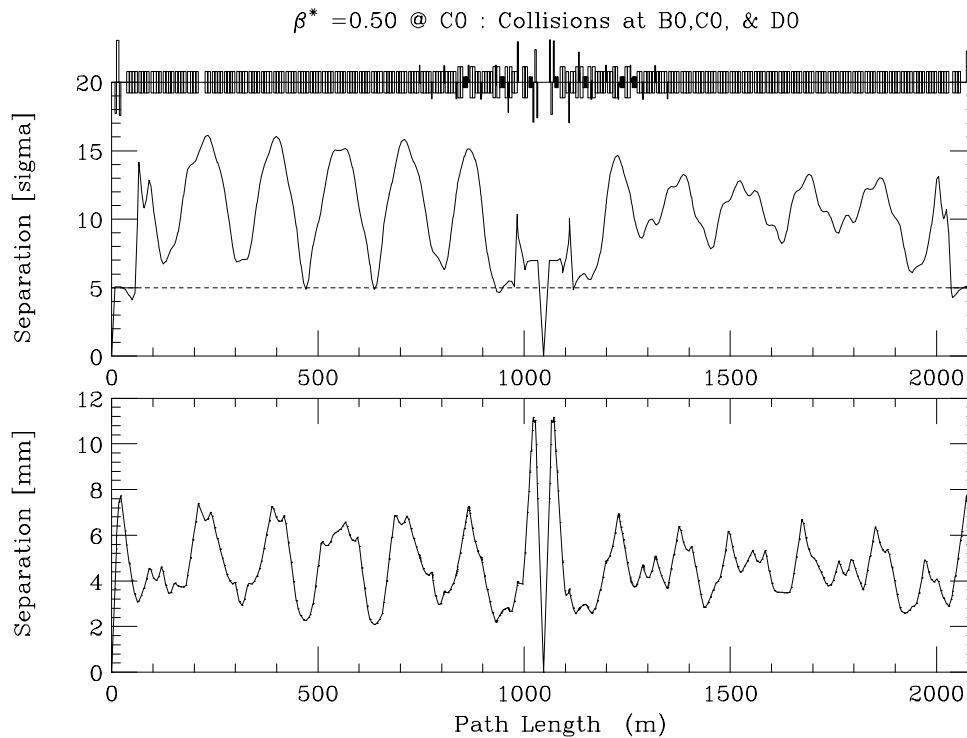
where $\theta_{1/2}$ is the total half-crossing angle, σ_{\parallel} is the rms bunch length, and σ_{\perp} is the rms transverse bunch size. For the purposes of the present discussion the relevant quantity is the transverse ratio $\theta_{1/2}/\sigma_{\perp}$. For "N" σ of separation at the first crossing this has the approximate value:

$$\frac{\theta_{1/2}}{\sigma_{\perp}} \approx \frac{N}{2\beta^*}$$

A β^* of 50 cm and 7σ separation at the 1st crossing, therefore, has an equivalent impact on luminosity as 5σ separation with $\beta^* = 35$ cm.

Separator gradients for this solution are listed in the table below, followed by the beam separation through the short arc B0 → C0 → D0. The very small gradients at B49 horizontally, and C11 vertically, are a further indication that the nominal helix is not a 'natural' candidate for C0 collision scenarios. One would prefer to see large kicks at these locations to initiate separation into the arcs.

Separator Gradients (MV / m)					
Horizontal			Vertical		
			B43	4	-2.14759
B46	4	3.00372			
B49	2	-0.48634	B49	1	-2.93754
C11	1	-3.24089	C11	2	0.60083
			C13	4	3.34755
C16	4	-1.75608			



3. AN IR WITH STANDARD TEVATRON DIPOLES

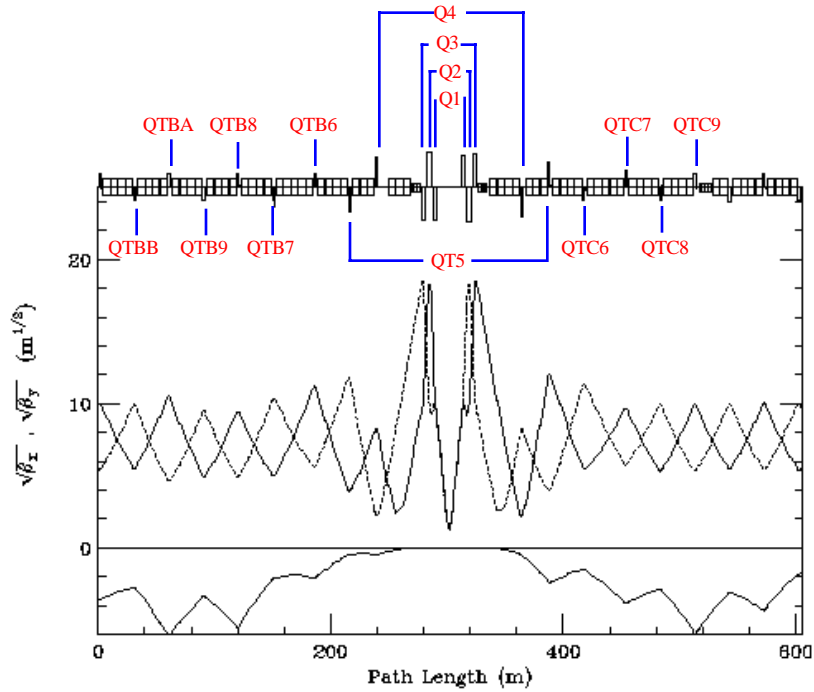
3.1. Physical Design

3.1.1. Quadrupoles

The IR quadrupole circuits, indicated on the following page, are identical to those described in the preceding section.

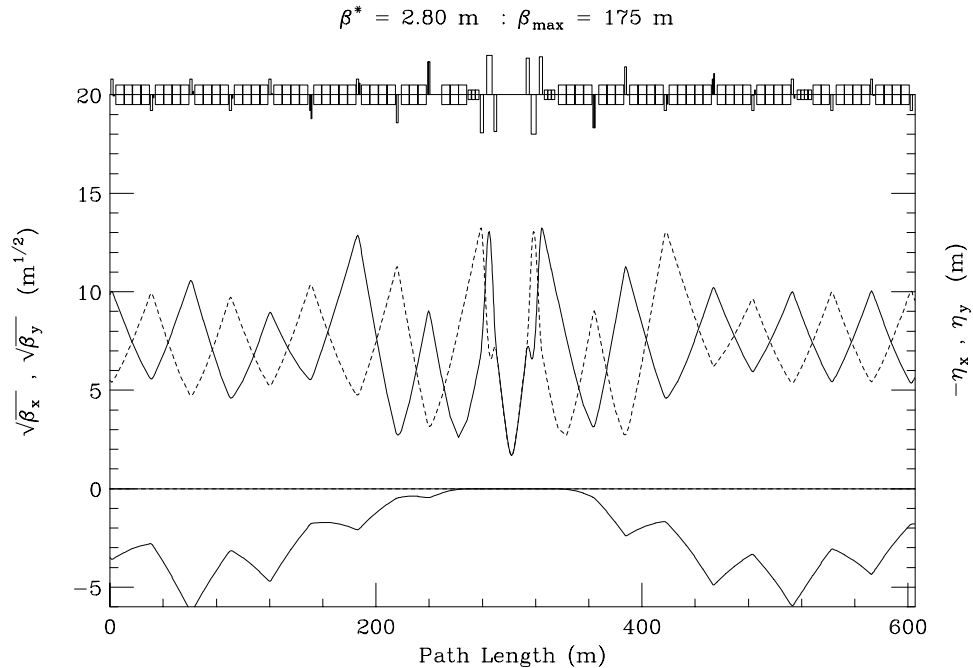
3.1.2. Dipoles & Separators

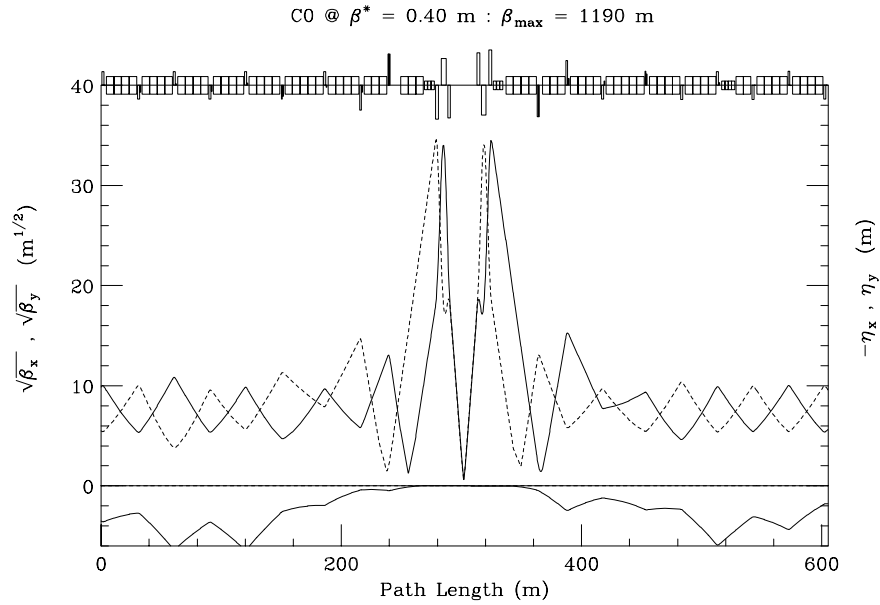
Having only standard Tevatron arc dipoles available for modelling has 2 significant consequences. First, it is not possible to add more separators in the arcs. Collisions at C0 can not be created without disrupting the nominal Run IIb helix outside of the insertion region. Second, the free space available for a detector shrinks markedly – by roughly $5^{1/2}$ m relative to the previous design – to just $33^{1/2}$ feet each side of the IP.



3.2. Optics

The injection & collision optics are illustrated in the next 2 graphs. At injection, $\beta^* = 2.80$ m results in a β_{max} of 175 m in the triplets. Again, this is much less than at B0 & D0. With the triplet quads closer to the IP in this version of the insert, a β^* as small as 40 cm can be reached before β_{max} becomes excessive. In all other respects the optical properties of this version of the IR are almost indistinguishable from those discussed in the preceding section. It would be odious, therefore, to present reams of nearly identical material again here.

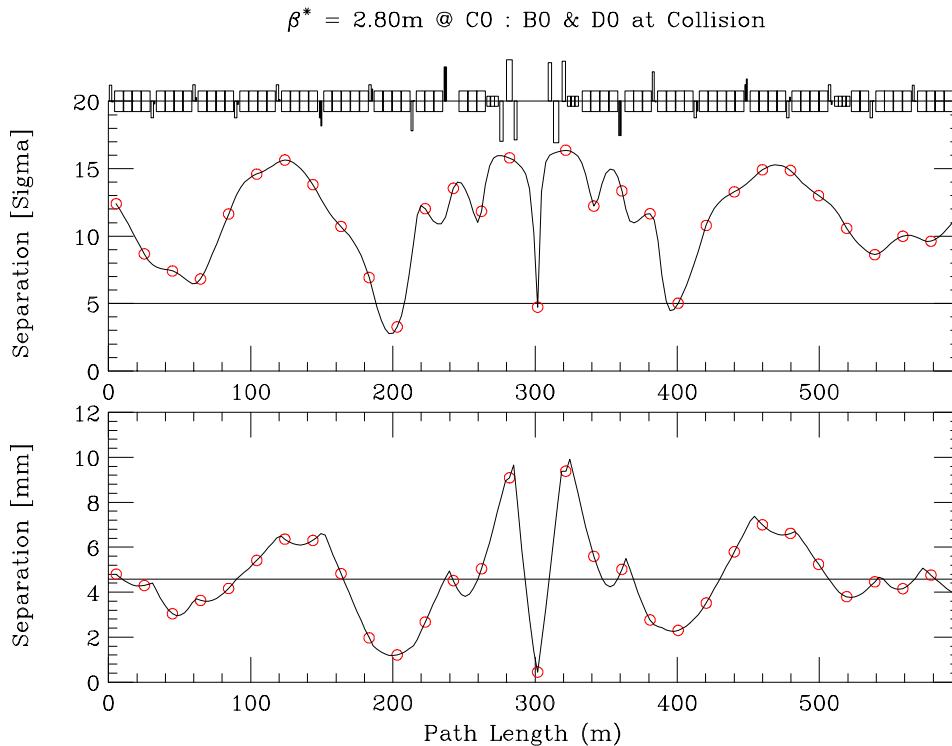




3.3. Beam Separation

With the restriction that C0 operations must not impact nominal Run IIb B0 & D0 collider parameters, and without additional separators, the Tevatron Collider can operate in just 2 modes:

- (1) B0 & D0 with collisions – not C0, and ;
- (2) C0 with collisions – not B0 & D0.



3.3.1. C0 Without Collisions

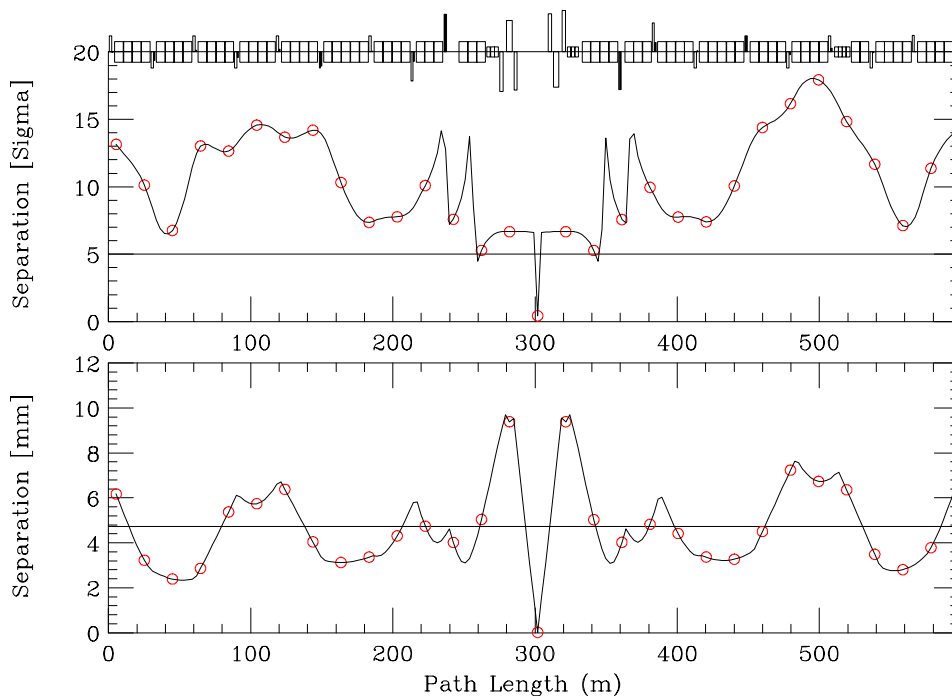
Without collisions at C0 the insertion optics are fixed at $\beta^* = 2.80$ m, and the B49 & C11 separators are turned off. The resulting matched helix from B38 \rightarrow C21 is shown on the preceding page. Beam separation is $\geq 5\sigma$ everywhere except for the 5th crossing point on B-Sector side. There is really nothing that can be done locally to influence this point – it is largely a feature of the nominal Run IIb helix.

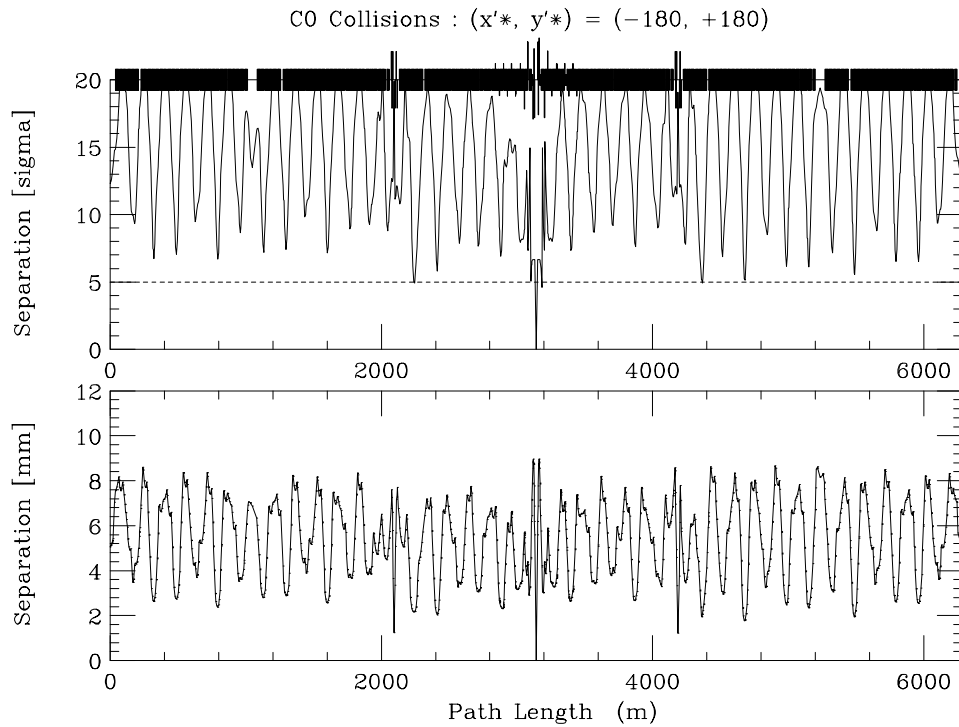
3.3.2. C0 With Collisions

For collisions at C0 the optics at B0 & D0 remain in their Injection configuration. In this case, all the separators in the ring become available for bringing beams together at the C0 IP, while keeping them separated everywhere else. For half-crossing angles at C0 of $(x^*, y^*) = (-180, +180)$ μ rad, one possible (minimal) separator solution is given in the table below. The selection of separators has not been optimized in any way, other than to ensure adequate beam separation around the ring. Many, many more combinations can be explored.

Separator Gradients (MV / m)					
Horizontal			Vertical		
			B11	1	-2.35261
B17	4	-0.102614			
B49	2	-4.50000	B49	1	4.50000
C11	1	4.50000	C11	2	-4.50000
			C17	4	-0.62098
C49	1	-1.35185			

$\beta^* = 0.40$ m : Collisions Only at C0



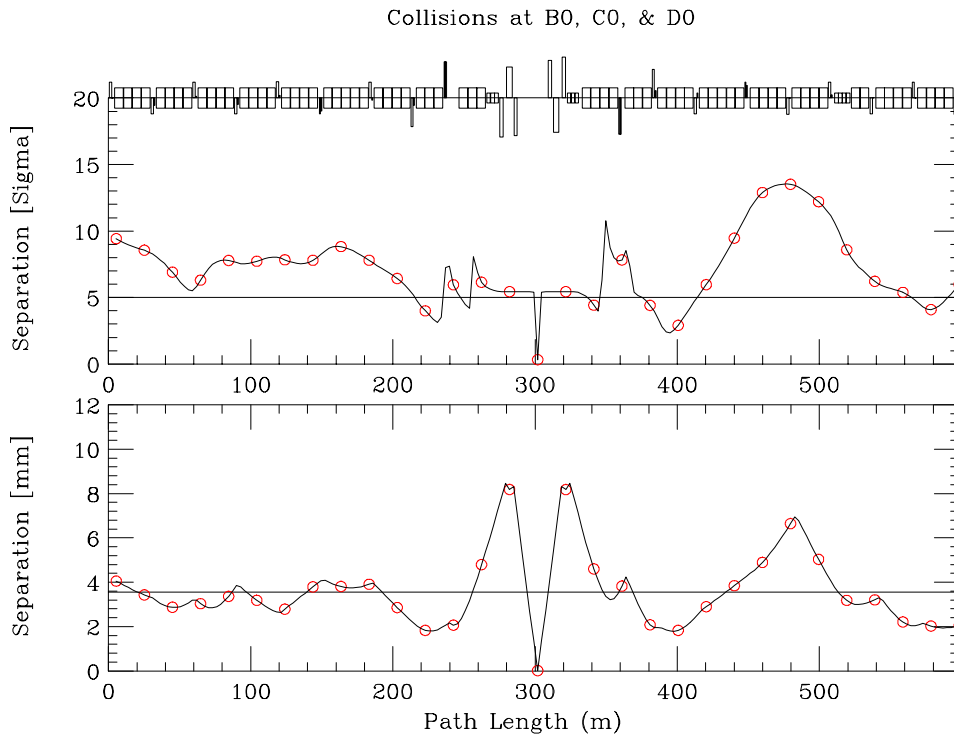


The preceding diagrams showed the beam separation from B38 → C21, and the separation all around the ring. With this separator solution the closest approach through the insert is at the 3rd parasitic crossing but, nonetheless, it is still $\geq 5\sigma$ everywhere. Similarly, separation in the ring drops close to 5σ in a few spots, but the average separation is $10 \rightarrow 15\sigma$. The use of a larger subset of separators would enable the large oscillations to be smoothed from the helix.

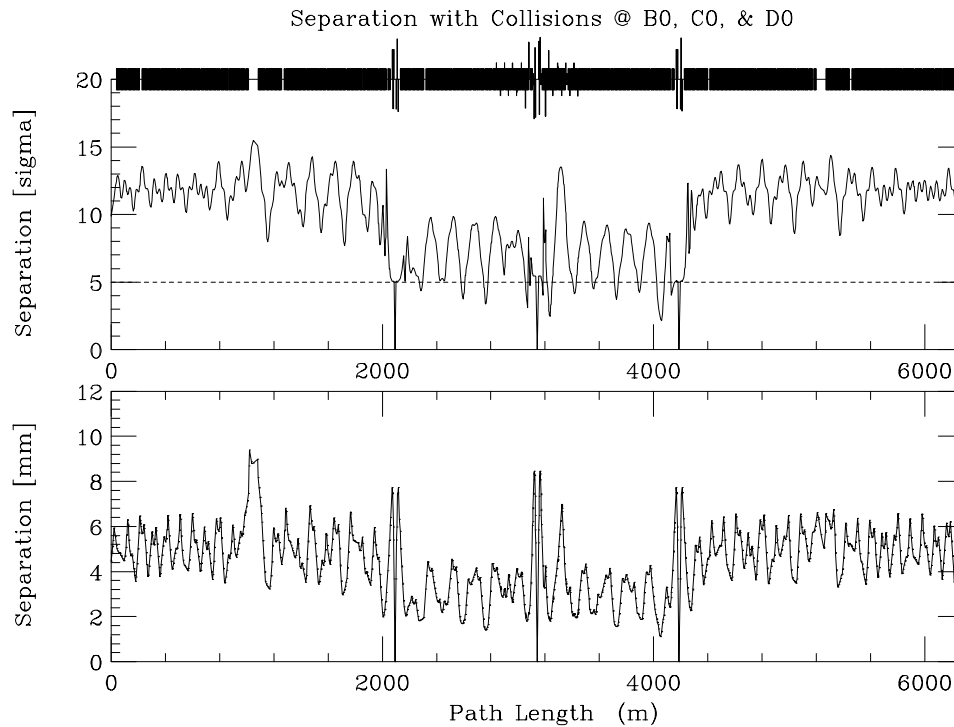
3.4. Collisions at B0, C0, & D0

In this version of the IR model, collisions can not occur at all 3 IP's consistent with the C0 insert remaining optically transparent. This section examines briefly, though, whether a reasonable 'semi-local' solution exists using only the separators in the short arc. There are 5 sets of separators, including the B49 & C11 modules, in each plane between B0 and D0. With the B0 & D0 crossing angles fixed at $(x'^*, y'^*) = (+170, -170) \mu\text{rad}$, and $(x'^*, y'^*) = (-180, +180) \mu\text{rad}$ at C0, only one separator solution exists with physically realizable gradients. Beam separation through the C0 insert & corresponding separator gradients for this case are shown below.

Separator Gradients (MV / m)					
Horizontal			Vertical		
B11	1	1.55253	B11	2	-2.93408
B17	4	-4.50000			
B49	2	2.55308	B49	1	-2.94817
C11	1	-2.28540	C11	2	-4.50000
			C17	4	3.57661
C49	2	-2.35765	C49	1	-2.30501



Splitting the crossing angle equally between the transverse planes optimizes beam separation into the arcs, but the solution obtained is clearly a very marginal situation. At several near-approach points through the insertion region beam separation drops below 5σ . The viability of this solution becomes even more suspect when separation in the short arc is compared with the rest of the ring (below). In going from $B0 \rightarrow C0 \rightarrow D0$ the separation is often less than 5σ , and average separation is only half that of the long arc $D0 \rightarrow E0 \rightarrow F0 \rightarrow A0 \rightarrow B0$.



4. Summary & Observations

Two possible conceptual optical designs for a stand-alone C0 IR insert were presented. Both inserts are optically transparent to the rest of the machine, with no impact on Run IIb Tevatron operating parameters. Both design variations require high-field LHC-like quadrupoles for the final focus triplet. In the first version, with enhanced dipoles creating space for separators in the arcs, collisions can be created at all 3 IP's simultaneously. Stronger dipoles also free more than 26 m of space for the detector. At C0, β^* is limited to ≥ 50 cm by β_{\max} in the IR triplets. The second version of the IR has neither new dipoles nor new arc separators. Collider scenarios have either B0 & D0 at collision, or just C0. At C0, β^* can be decreased to 40 cm, but the price paid is a substantial reduction in free space available for the detector.

This first pass at C0 IR designs has left a number of questions unresolved. A few of these outstanding issues that a second iteration of the IR designs must address are discussed below.

- The LHC-like quadrupoles operate with gradients somewhat higher than the present Tevatron cryogenics can tolerate. Reducing the strengths will require that the magnets become longer. If gradients are kept ≤ 175 T/m, the magnetic lengths of the triplet quads Q1, Q2, & Q3 are estimated to grow by $\sim 5\%$, and Q4 by $\sim 10\%$, for a total of $\approx 24''$. Both IR versions discussed here can easily accommodate these changes without encroaching on the detector space. In the IR model with enhanced dipoles a total of $17'$ of free space currently exists between the downstream separators & Q4. The design with only standard Tevatron dipoles has $5\frac{1}{4}'$ between the separators & first dipole. In the model at least, length changes become just a technical detail.
- The addition of a new low- β has a huge impact on chromaticity, changing the natural chromaticity of the machine by $(\Delta\nu_x, \Delta\nu_y) = (-19.75, -19.70)$. If the insertion is to be truly transparent a local sextupole correction scheme must be devised for compensation.
- With all 3 IP's at collision beam separation through the C0 IR is not as large as desired. Partly this is a consequence of the current Run IIb helix not being optimized in any way to account for C0 interactions. A comparison of separation through the insert with B0, C0, & D0 collisions (section 2.3), with just C0 collisions (section 3.3.2), shows the large improvement in beam separation that can result with a different incoming helix. The options for alternative, global, separator solutions that optimize the collision helix for B0 & D0, plus C0, should be explored.

